

This is the accepted manuscript made available via CHORUS. The article has been published as:

## Quantifying Screening Ion Excesses in Single-Molecule Force-Extension Experiments

Jonathan Landy, D. B. McIntosh, and O. A. Saleh

Phys. Rev. Lett. **109**, 048301 — Published 23 July 2012

DOI: [10.1103/PhysRevLett.109.048301](https://doi.org/10.1103/PhysRevLett.109.048301)

# Quantifying screening ion excesses in single-molecule force-extension experiments

Jonathan Landy,<sup>1,\*</sup> D. B. McIntosh,<sup>2,†</sup> and O. A. Saleh<sup>1,3,‡</sup>

<sup>1</sup>*Materials Department, University of California, Santa Barbara, CA 93106, USA*

<sup>2</sup>*Physics Department, University of California, Santa Barbara, CA 93106, USA*

<sup>3</sup>*BMSE program, University of California, Santa Barbara, CA 93106, USA*

(Dated: June 10, 2012)

We derive a thermodynamic identity that allows one to infer the change in the number of screening ions that are associated with a charged macromolecule as the macromolecule is continuously stretched. Applying this identity to force-extension data on both ss and dsDNA, we find that the number of polymer-associated ions depends non-trivially on both the bulk salt concentration and the bare rigidity of the polymer, with ssDNA exhibiting a relatively large decrease in ion excess upon stretching. We rationalize these observations using simple models for polyelectrolyte extension.

In the crowded environment of the cell, biological macromolecules are constantly surrounded by many smaller molecules with which they interact and become associated [1]. The resulting dressed macromolecules may be described by a set of renormalized, or effective, mechanical and chemical properties that determine larger-scale behavior. A challenging first step towards characterizing these properties is the quantitative identification of the constituents of the complexes, which, being small, are generally difficult to directly measure.

One way to circumvent measurement difficulty is to indirectly probe quantities of interest via the application of identities relating those quantities to others that are more readily measurable. Recent efforts along these lines have focused on thermodynamic Maxwell identities that can be applied to determine protein binding numbers on stretched DNA [1–3]. In this Letter, we extend these considerations to the case of the screening of stretched, charged macromolecules. This scenario differs significantly from the case of protein binding in that the associated molecules (screening ions, in this case) are not each directly bound to the macromolecule. Nevertheless, by treating these ions using the concept of molecular excess [4], we derive a corresponding Maxwell identity that relates changes in a macromolecule’s extension to changes in the number of macromolecule-associated ions (including both diffuse and condensed screening ions). We apply this identity to single-molecule measurements of the force-extension behavior of both single- and double-stranded (ss/ds)DNA. This allows us to explore quantitatively – via a model-free analysis of experimental data – how the makeup of polymer/screening cloud complexes changes as a function of ionic environment, bare rigidity, and net extension. While both bulk [5] and single-molecule [6] measurements of ionic excesses have been carried out previously, the methods employed have been limited – in the bulk case by the lack of control over macromolecular configuration, and in the single-molecule case to changes in excess across discrete transitions (e.g. condensation, using Clausius-Clapeyron relations). In contrast, the single-molecule method that we demonstrate here allows for both direct and continuous control

over macromolecular conformation, and it thus allows for the characterization of excesses in general states.

We consider an isolated macromolecule (shown as a polyelectrolyte in Fig. 1) that sits within an infinite bulk solution. A force  $f$  is applied at one end, while the other end is held fixed. We treat the system by considering a large, fixed volume  $V$  (which can formally be taken to infinity) that surrounds the entirety of the macromolecule/screening cloud complex. The grand partition sum for this volume is then

$$\mathcal{Z} = \sum_{\{N_i\}} \int_X e^{-\beta(F_{int}(X, \{N_i\}) - fX - \sum_i \mu_i N_i)}, \quad (1)$$

where  $X$  is the end-to-end extension of the macromolecule,  $N_i$  is the number of molecules of species  $i$  contained within the volume, and  $F_{int}$  is the internal free energy of the volume at fixed  $X$  and  $\{N_i\}$ . At constant temperature and pressure, the chemical potentials in (1) are interrelated through the bulk’s Gibbs-Duhem equation,  $\sum_i c_i d\mu_i = 0$ , where  $c_i$  is the bulk concentration of molecular species  $i$  [4]. Choosing the set of solute chemical potentials as our independent basis set, this equation slaves the solvent chemical potential  $\mu_W$  (water in our experiments) to those of the solutes, and we obtain

$$d\mathcal{F}|_{T,V} = -\langle X \rangle df - \sum_i \langle n_i \rangle d\mu_i, \quad (2)$$

where  $\beta\mathcal{F} \equiv -\log \mathcal{Z}$ . Here, brackets have been used to denote a thermal average, the sum on the right is now over solute species only, and  $n_i$ , the molecular excess of species  $i$ , is given by

$$\begin{aligned} n_i &\equiv N_i - \frac{c_i}{c_W} N_W \\ &= N_i - c_i V - \frac{c_i}{c_W} \{N_W - c_W V\}. \end{aligned} \quad (3)$$

The bracketed, third term here will generally take on non-zero values due to the finite size of the solute particles, which, if present in excess, should expel water from the macromolecule’s surroundings because of excluded volume effects. However, because this term is proportional

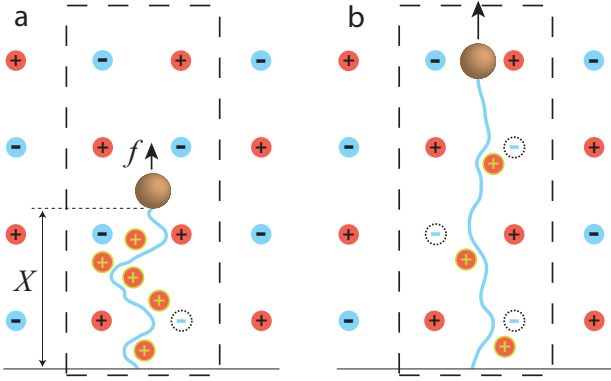


FIG. 1: (color online) Anionic polyelectrolyte in a magnetic tweezers assay in equilibrium with a bulk salt bath (not to scale). At the boundary of the volume considered (dashed rectangles), the local ionic environment is indistinguishable from the bulk. (a) At low forces, the high charge density of the compact polymer attracts additional cations (shown highlighted in yellow) and repels some anions, creating anion “holes” (shown with dashed border); these ions and “holes” compose the two excesses. (b) At higher forces, some cations are released into the bulk, along with pairing anions to maintain charge neutrality.

to  $c_i/c_W$ , the first two terms generally dominate in (3), and one can often think of the excess as the number of molecules of species  $i$  near the macromolecule minus the number that would be present if the macromolecule were absent. This value can be positive, negative, or zero.

We now specialize to the case where the only added solute is a binary salt with counterion valence  $Z_1$  and coion valence  $Z_0 = -1$ . Charge neutrality of the bulk requires that the counterion and coion concentrations satisfy  $Z_1 c_1 = c_0$ . At equilibrium, these bulk concentrations set the chemical potentials of these species through

$$\mu_i = k_B T \log(\gamma_i c_i), \quad (4)$$

where  $\gamma_i$  is a species-dependent activity coefficient. The averaged excesses are related through the charge neutrality condition that holds for the complex,

$$-Q_0 + \sum_i Z_i \langle n_i \rangle = 0, \quad (5)$$

with  $-Q_0 e$  the bare charge of the polymer. Using these results, equating the mixed partials of  $\mathcal{F}$  in (2) gives

$$\beta \partial_{c_1} \langle X \rangle|_{T,f} = \mathcal{A} \left( \frac{1 + Z_1}{c_1} \right) \partial_f \langle n_1 \rangle|_{T,c_1}, \quad (6)$$

where  $\mathcal{A} \equiv 1 + \frac{c_1}{Z_1 + 1} \partial_{c_1} \log(\gamma_1 \gamma_0^{Z_1})$ . This is our main theoretical result. Given knowledge of  $\langle X \rangle \equiv \langle X(f, c_1) \rangle$ , the Maxwell identity (6), together with (5), allows one to infer the changes in the  $\langle n_i \rangle$  as  $f$  is varied. Henceforth, we focus on monovalent salt and refer to the change in the excesses as  $\Delta n = \Delta \langle n_0 \rangle = \Delta \langle n_1 \rangle$ , for brevity.

We turn now to a discussion of our experimental setup and results. We create bifunctional dsDNA by annealing and ligating 5'-phosphorylated, 3'-digoxigenin or biotin labeled DNA oligomers (MWG Biotech) to the cosquences of lambda DNA (NEB). Synthesis of permanently denatured, bifunctional ssDNA has been described elsewhere [7, 8]. Single polymers (48.5 kbp lambda DNA, and 10.5 kb ssDNA) are stretched in a magnetic tweezers assay as discussed in [9]. Briefly, single polymers are immobilized to a glass cover slip in a flow cell via the digoxigenin moiety, and a micron-sized paramagnetic bead is attached to the free end via the biotin moiety (see Fig. 1). External magnets are moved above the sample to control the force while the bead position is tracked in real time. The force is calibrated as a function of magnet position by measuring the fluctuations of the bead [9]. Once calibrated, the force-extension behavior is measured at various salt concentrations by measuring the bead height while varying the magnet position (see Figs. 2a,b). dsDNA is stretched in the presence of tris buffer (which contains only monovalent ions), pH 7.5, at ionic strengths of 0.4 – 8 mM. ssDNA is stretched in solutions containing 50 – 1000 mM NaCl with a background of 10 mM tris buffer (ionic strength 8 mM, pH 7.5), which we assume to be negligible for the purposes of counting excess ions.

Figs. 2c and 2d show the change in ion excess as computed from the measured force-extension data for ssDNA and dsDNA, respectively. In order to generate these plots, we first carried out global, low order polynomial fits in  $\log c_1$  and  $\log f$  to individual strand force-extension data sets (example fits are shown as the solid curves in Figs. 2a, b) [22]. This provided us with a smooth fit function  $X(f, c_1)$  for each strand that could be plugged into (6) and then integrated over  $f$ . The factor  $\mathcal{A}$  was evaluated both through the use of the ideal assumption ( $\mathcal{A} = 1$ , solid curves) and also through the use of the modified-Davies equation introduced in [10] (dashed curves), which gives accurate ion activity coefficient values for binary monovalent salts at or below one molar concentration. Data acquisition for this application was challenging, particularly for dsDNA at high force where the force-extension curves change by only 10's of nanometers across concentrations. Thus, relatively small offsets in any given force-extension curve can lead to clearly unphysical results upon integration of  $\partial_{c_1} \langle X \rangle$ . A minority of the acquired data sets displayed such behavior and were removed from our analysis. In all, the computed excess versus force plots represent averages across thirteen of sixteen acquired dsDNA data sets and five of six acquired ssDNA data sets. In both cases, the excess is plotted only over the force range in which the different concentration curves are well-separated [23].

There are various qualitative features of interest present in Figs. 2c and 2d. First, we see that in both cases, the excess is a decreasing function of force (and, hence, extension). For ssDNA, the ionic excess decreases

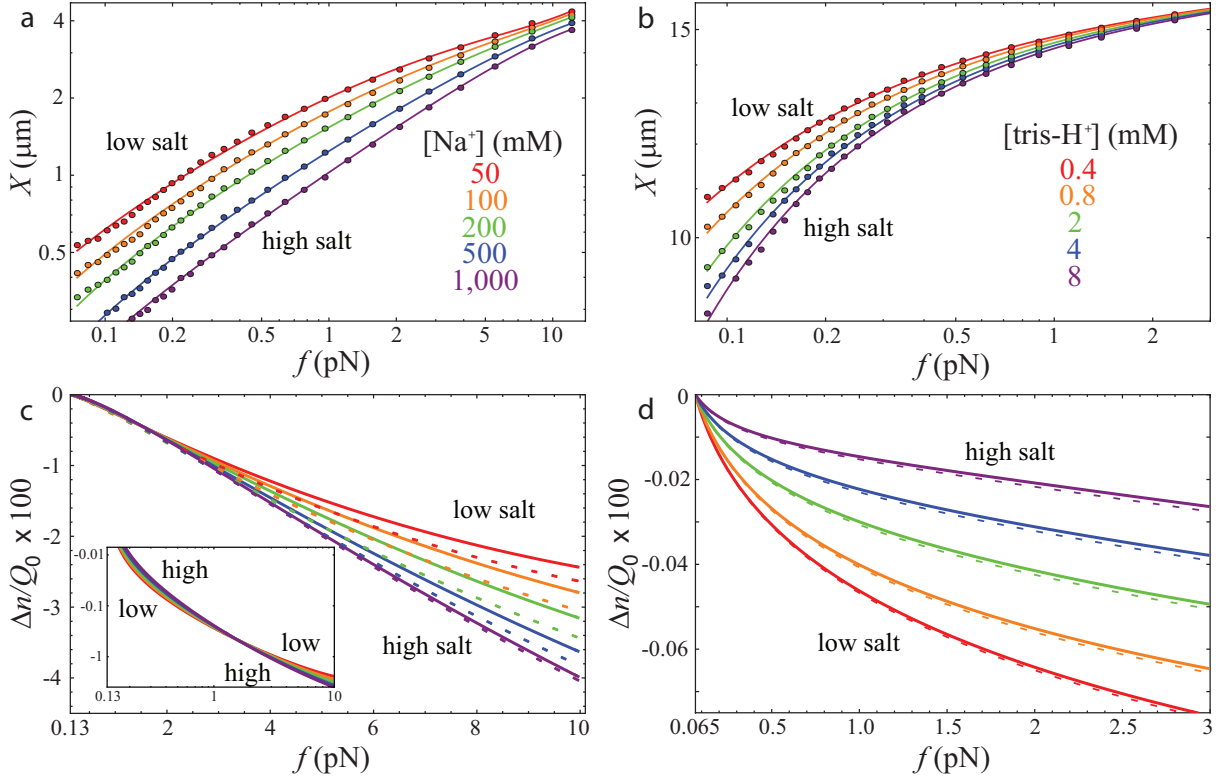


FIG. 2: (color online) (a,b): Log-log plot of force-extension data for a single ssDNA strand (a) and for a single dsDNA strand (b) across multiple monovalent salt concentrations,  $c_1$  (fits in solid line). (c,d): The change in ionic excess  $\Delta n$  versus force at different  $c_1$  for ssDNA (c) and dsDNA (d) (relative to values at  $f = 0.13$  pN and  $f = 0.065$  pN for ssDNA and dsDNA, respectively). The change in excess is normalized by the total number of strand phosphates  $Q_0$  and is multiplied by a factor of 100. Solid lines do not include activity coefficient corrections (i.e.  $\mathcal{A} \rightarrow 1$ ), while the dashed lines do. ssDNA, a flexible polyelectrolyte, exhibits a crossover in concentration dependence as one moves from low to high forces as shown in the log-log inset to (c). Over the force range considered, dsDNA is always in the high force limit ( $fl_p \gg k_B T$ ), and the concentration dependence is opposite to that observed for ssDNA in the same limit.

by a few percent of the total number of bare strand charges over the force range considered (e.g. at 100 mM,  $\Delta n \approx -250$ , with  $Q_0 \approx 10^4$ ). For dsDNA, the decrease in excess is only significant at relatively low salt concentrations, and even then is often smaller than that for ssDNA. For example, at the concentrations considered in Fig. 2d the relative decrease is at most 0.1% of the total charge (e.g. at 8 mM,  $\Delta n \approx -100$ , with  $Q_0 \approx 10^5$ ). In both cases, however, the entropy gained through ion release is significant [24]. A decrease in excess with extension is to be expected: When a polymer is in its globule state, its charge is localized in space, and this leads to relatively strong electric fields. Non-linear screening effects become more significant at strong field strengths, and this leads to an increase in ion association with the polymer. This effect is known to help stabilize RNA tertiary structure, for example [11]. In addition, when a polymer has some slack, conformational fluctuations are expected to result in a degree of source charge heterogeneity, which also leads to an increase in charge condensation through certain non-linear screening mechanisms [12, 13]. Both ef-

fects are reduced upon stretching, and this should result in a degree of counterion/coion release, as observed.

A second notable feature of the data is that, in the high force limit, the magnitude of  $\Delta n$  increases with  $c_1$  for ssDNA, but decreases with  $c_1$  for dsDNA. This can be qualitatively understood through the OSF theory of polyelectrolyte behavior, which predicts that the effective persistence length of a charged polymer should scale as  $l_p = l_0 + l_e$ , with  $l_0$  a bare, mechanical contribution and  $l_e \sim A c_1^{-\alpha}$  an electrostatic, salt concentration-dependent contribution [14, 15]. This form can be plugged into the worm-like chain model of polymer elasticity, which at high forces ( $fl_p \gg k_B T$ ) gives an extension of [16]

$$\frac{X}{L} \approx 1 - \frac{1}{2} \sqrt{\frac{k_B T}{fl_p}}, \quad (7)$$

where  $L$  is the chain contour length. This high force limit applies for dsDNA above  $\sim 0.1$  pN [16], and crudely describes ssDNA above  $\sim 1$  pN [8]. Plugging this form

into (6), we obtain

$$\Delta n = -\frac{l_e}{l_p^{3/2}} \times \frac{\alpha L}{4A} \sqrt{\frac{f}{k_B T}}, \quad (8)$$

which gives values for  $\Delta n$  that are roughly twice those that appear in Figs. 2c and 2d [25] (capturing the  $\approx 30$ -fold difference in order of magnitude between ssDNA and dsDNA). The factor  $l_e l_p^{-3/2}$  dominates the concentration dependence in (8), and the qualitative differences between ssDNA and dsDNA can be understood in terms of the scaling of this term. For ssDNA,  $l_p \approx l_e$  because  $l_e \gg l_0$  throughout the concentration range considered [7]. Consequently, within this model  $\Delta n \propto c_1^{\alpha/2}$ , an increasing function in  $c_1$ , as observed. On the other hand, in the concentration regime considered, dsDNA is dominated by its intrinsic rigidity,  $l_p \approx l_0$ . In this limit,  $\Delta n \propto c_1^{-\alpha}$ , a decreasing function in  $c_1$ , again as observed.

At low forces ( $\lesssim 1$  pN), the extension of ssDNA depends upon the salt concentration through both the excluded volume parameter  $v$  and the persistence length  $l_p$ , scaling as [8, 17]

$$X \sim L \left( \frac{v}{l_p} \right)^{1/3} \left( \frac{f}{T} \right)^{2/3}. \quad (9)$$

Previous analysis [7] indicates that, as before,  $l_p \sim A c_1^{-\alpha}$ , and also that  $v \sim B c_1^{-\beta}$ , with  $\beta > \alpha$ . Plugging into the Maxwell relation (6) we obtain  $\Delta n \propto c_1^{(-\beta+\alpha)/3}$ . Because  $\beta > \alpha$ , it follows that  $\Delta n$  is expected to decrease with  $c_1$  at low forces. A low-force turnover in concentration dependence is, in fact, observed in the experimental results, as highlighted in the inset of Fig. 2c. Thus, each of the main qualitative features of Figs. 2c, d appear to be consistent with those one would obtain using familiar models of polyelectrolyte statistics, together with (6).

To summarize, we have developed a framework combining the Gibbs-Duhem and Maxwell relations (Eqs. 2 and 3) that allows for quantification of the change in excess of any macromolecule-associated solute from single-molecule force-extension curves; this could be applied to a variety of stretching experiments in which the chemical potential of a solute is varied [18, 19]. Here, we have particularly focused on quantifying excess salt ions by deriving and applying the Maxwell relation (6). Using this identity, we have obtained quantitative measures for changes in the ionic excess for stretched DNA in monovalent salt, and we have found that the results can be qualitatively understood through the use of simple models for polyelectrolyte extension. In particular, we have found that the excess changes rapidly for ssDNA as its extension is continuously adjusted, a result that we expect to hold for all flexible polyelectrolytes, including RNA.

We thank Philip Pincus for helpful discussions. This work was partially supported by the NSF through grants DMR-1006737 and DMR-1101900.

\* Electronic address: [landy@mrl.ucsb.edu](mailto:landy@mrl.ucsb.edu)

† Electronic address: [dmcintos@physics.ucsb.edu](mailto:dmcintos@physics.ucsb.edu)

‡ Electronic address: [saleh@engineering.ucsb.edu](mailto:saleh@engineering.ucsb.edu)

- [1] H. Zhang and J. F. Marko, Phys. Rev. E **77**, 031916 (2008).
- [2] B. Xiao, R. C. Johnson, and J. F. Marko, Nucl. Acids Res. **38**, 6176 (2010).
- [3] B. Xiao, H. Zhang, R. C. Johnson, and J. F. Marko, Nucl. Acids Res. **39**, 5568 (2011).
- [4] V. A. Parsegian, R. P. Rand, and D. C. Rau, Proc. Natl. Acad. Sci. USA **97**, 3987 (2000).
- [5] Y. Bai, M. Greenfield, K. J. Travers, V. B. Chu, J. Lipfert, S. Doniach, and D. Herschlag, J. Am. Chem. Soc. **129**, 14981 (2007), and references therein.
- [6] B. A. Todd and D. C. Rau, Nucl. Acids Res. **36**, 501 (2008).
- [7] O. A. Saleh, D. B. McIntosh, P. Pincus, and N. Ribeck, Phys. Rev. Lett. **102**, 068301 (2009).
- [8] D. B. McIntosh, N. Ribeck, and O. A. Saleh, Phys. Rev. E **80**, 041803 (2009).
- [9] N. Ribeck and O. A. Saleh, Rev. Sci. Instrum. **79**, 094301 (2008), and references therein.
- [10] E. Samson, G. Lemaire, J. Marchand, and J. J. Beaudoin, Computational Materials Science **15**, 285 (1999).
- [11] D. E. Draper, RNA **10**, 335 (2004).
- [12] D. B. Lukatsky, S. A. Safran, A. W. C. Lau, and P. Pincus, Europhys. Lett. **58**, 785 (2002).
- [13] J. Landy, Phys. Rev. E **81**, 011401 (2010).
- [14] T. Odijk, J. Polym. Sci., Part B: Polym. Phys. **15**, 477 (1977).
- [15] J. Skolnick and M. Fixman, Macromolecules **10**, 944 (1977).
- [16] J. F. Marko and E. D. Siggia, Macromolecules **28**, 8759 (1995).
- [17] P. Pincus, Macromolecules **9**, 386 (1976).
- [18] C. Liu, Z. Wang, and X. Zhang, Macromolecules **39**, 3480 (2006).
- [19] I. Popa, B. Zhang, P. Maroni, A. D. Schlter, and M. Borkovec, Angew. Chem. Int. Ed. **49**, 4250 (2010).
- [20] J. Landy, D. B. McIntosh, O. A. Saleh, and P. Pincus (2012), to be published.
- [21] J.-L. Barrat and J.-F. Joanny, Europhys. Lett. **24**, 333 (1993).
- [22] We have found the resulting excess versus force plots to be insensitive to the fitting form used, provided the fits go through the data points in a reasonably smooth manner. The fits shown in Fig. 2 are third order polynomials in  $\log f$ , with coefficients that are themselves second order polynomials (with fitting parameter coefficients) in  $\log c$ .
- [23] The curves are well-separated in the sense that the mean curves for each concentration (those shown in Figs. 2c,d) each fall outside the one standard deviation uncertainty window (corresponding to the observed variation across retained data sets) for each other concentration curve.
- [24] Estimates indicate that the change in mobile ion entropy is  $\approx 30$  percent of the total free energy difference between the globule and extended states for both ss and dsDNA at the salt concentrations considered here [20].
- [25] Values that converge at large  $f$  (and that are closer to our experimental results) can be obtained through the use of more realistic models, such as that of [21].